Predicting central lymph node metastasis in papillary thyroid cancer: A nomogram based on clinical, ultrasound and contrast-enhanced computed tomography characteristics

QIANRU ZHANG[1*], SHANGYAN XU[1*], QI SONG[2], YUANYUAN MA[2], YAN HU[1], JIEJIE YAO[1] and WEIWEI ZHAN[1]

[1]Department of Ultrasound, Ruijin Hospital, Shanghai Jiao Tong University School of Medicine, Shanghai 200025, P.R. China; [2]Department of Radiology, Ruijin Hospital, Shanghai Jiao Tong University School of Medicine, Shanghai 200025, P.R. China

Received February 2, 2024; Accepted July 12, 2024

DOI: 10.3892/ol.2024.14611

Abstract. Central lymph node (CLN) status is considered to be an important risk factor in patients with papillary thyroid carcinoma (PTC). The aim of the present study was to identify risk factors associated with CLN metastasis (CLNM) for patients with PTC based on preoperative clinical, ultrasound (US) and contrast-enhanced computed tomography (CT) characteristics, and establish a prediction model for treatment plans. A total of 786 patients with a confirmed pathological diagnosis of PTC between January 2021 to December 2022 were included in the present retrospective study, with 550 patients included in the training group and 236 patients enrolled in the validation group (ratio of 7:3). Based on the preoperative clinical, US and contrast-enhanced CT features, univariate and multivariate logistic regression analyses were used to determine the independent predictive factors of CLNM, and a personalized nomogram was constructed. Calibration curve, receiver operating characteristic (ROC) curve and decision curve analyses were used to assess discrimination, calibration and clinical application of the prediction model. As a result, 38.9% (306/786) of patients with PTC and CLNM(-) status before surgery had confirmed CLNM using postoperative pathology. In multivariate analysis, a young age (≤45 years), the male sex, no presence of Hashimoto thyroiditis, isthmic location, microcalcification, inhomogeneous enhancement and capsule invasion were independent predictors of CLNM in patients with PTC. The nomogram integrating these 7 factors exhibited strong discrimination in both the training group [Area under the curve (AUC)=0.826] and the validation group (AUC=0.818). Furthermore, the area under the ROC curve for predicting CLNM based on clinical, US and contrast-enhanced CT features was higher than that without contrast-enhanced CT features (AUC=0.818 and AUC=0.712, respectively). In addition, the calibration curve was appropriately fitted and decision curve analysis confirmed the clinical utility of the nomogram. In conclusion, the present study developed a novel nomogram for preoperative prediction of CLNM, which could provide a basis for prophylactic central lymph node dissection in patients with PTC.

Correspondence to: Professor Weiwei Zhan or Professor Jiejie Yao, Department of Ultrasound, Ruijin Hospital, Shanghai Jiao Tong University School of Medicine, 197 2nd Ruijin Road, Shanghai 200025, P.R. China
E-mail: shanghairuijin@126.com
E-mail: jannyfulyao@126.com

*Contributed equally

Abbreviations: PTC, papillary thyroid cancer; CLNM, central lymph node metastasis; CLND, central lymph node dissection; US, ultrasound; CT, computed tomography; ROC, receiver operating characteristic; DCA, decision curve analysis; AUC, area under the curve; TSH, thyroid stimulating hormone; TG, thyroglobulin; TGAb, TG antibody; TPOAb, thyroid peroxidase antibody; OR, odd ratio; CI, confidence interval

Key words: CLNM, PTC, ultrasound, contrast-enhanced CT, prediction nomogram

Introduction

Thyroid cancer, a malignancy ranking ninth worldwide in terms of incidence, can occur in people of any sex and any age (1). Papillary thyroid cancer (PTC) is the predominant type of thyroid cancer, making up ~80% of cases (2). Despite a more favorable overall prognosis compared with other forms of thyroid cancer (3), patients with PTC are more likely to have central lymph node metastasis (CLNM), and the incidence of CLNM is 30-80% (4,5), which is considered to be the most important risk factor of regional recurrence and poor survival (6). Therefore, to achieve the goal of radical tumor resection, surgeons will often perform therapeutic central lymph node dissection (CLND) in patients with PTC (7). However, it is still controversial as to whether CLN dissection should be performed in patients with PTC with clinically negative (cN0) CLNM. Certain cN0 patients have potential CLNM, therefore prophylactic CLND can lower the rate of postoperative regional recurrence rate and avoid a second surgery (8,9). However, prophylactic CLND is not particularly

cost-effective, and the risk of recurrent laryngeal nerve injury, permanent hypoparathyroidism and other associated complications is greatly increased (10). Furthermore, ultrasound (US)-guided ablation is a safe, effective and minimally invasive substitute for surgical resection for patients with low-risk PTC without CLNM (11). Therefore, it is important to evaluate the central lymph nodes accurately and comprehensively before operation to avoid overtreatment and undertreatment, and to provide a more reasonable surgical plan for patients.

Given its non-invasiveness, non-radiation and high resolution, US is the preferred preoperative imaging technique for assessing thyroid nodules and cervical lymph nodes. It can clearly show the tumor size, location, shape, margin, composition, echogenicity, microcalcification and blood flow signal (12,13). However, owing to the influence of the anatomical structures of the central neck, the effect of US in detecting CLNM is not ideal (4,14). Meanwhile, US is also limited by the reliance on operator skills and the incapacity to visualize deep structures (15). Therefore, the American Thyroid Association guidelines recommend contrast-enhanced computed tomography (CT) as an adjunct to US to improve the accuracy of preoperative diagnosis (7). Contrast-enhanced CT effectively avoids the shortcomings of US. First, contrast-enhanced CT can provide comprehensive cross-sectional images of the thyroid gland and neighboring structures including the trachea, esophagus, blood vessels and lymph nodes (16,17). Second, due to the absence of gas and bone restrictions, contrast-enhanced CT may better visualize lymph node metastasis, capsule invasion and extrathyroidal extension (18-20).Therefore, the combination of US and contrast-enhanced CT diagnosis would be complementary, to make up for the deficiency of the single application of contrast-enhanced CT or US for diagnosing thyroid nodules, and improve the diagnostic specificity and sensitivity.

Currently, most studies predicting CLNM in patients with PTC have focused on clinical and US features, and the results are consistent (21-23). Furthermore, to the best of our knowledge, few studies have investigated the association between contrast-enhanced CT features and CLNM in patients with PTC. Therefore, the present study used contrast-enhanced CT features to determine the risk factors for CLNM in patients with cN0 PTC, aiming to identify key predictors and establish a new nomogram for predicting the risk of CLNM in patients with PTC to facilitate preoperative decision making for prophylactic CLND.

Materials and methods

Patients selection. Owing to the retrospective study design, approval from the Ethics Committee of Ruijin Hospital, Shanghai Jiao Tong University School of Medicine (Shanghai, China) was obtained and the requirement for informed consent was waived.

A total of 6,275 patients who underwent thyroidectomy along with CLND and were histopathologically confirmed to have PTC at Ruijin Hospital from January 2021 to December 2022 were enrolled in the present study. The inclusion criteria were as follows: i) Treatment with primary thyroid surgery and CLND, and a BRAF V600E mutation test; ii) histopathologically confirmed PTC; iii) no signs of lymph node metastasis (cN0), conventional US and contrast-enhanced CT performed, and a medical history collection within 3 weeks before surgery; iv) preoperative thyroid function tests performed and no prior history of thyroxine treatment [including thyroid stimulating hormone (TSH), thyroglobulin (TG), TG antibody (TGAb) and thyroid peroxidase antibody (TPOAb)]; and v) only the largest nodule was included for patients with multiple nodules (with at least two of which confirmed as PTC). Exclusion criteria were as follows: i) Tumor size of <0.5 cm; ii) treatment of head and neck radiotherapy therapy; iii) presence of other malignant tumors, such as nasopharyngeal carcinoma and breast cancer; iv) incomplete or low quality medical records; and v) inconsistent imaging tumor lesions with the pathological results. Based on the aforementioned inclusion and exclusion criteria, the data from 786 patients with cN0 PTC were analyzed in the present study. The flowchart depicting the selection process is presented in Fig. 1.

US assessment. All participants were evaluated using US equipment (MyLab™ 9, Esaote S.p.A; DC-8, Shenzhen Mindray Bio-Medical Electronics Co., Ltd.; and iU22, Philips Medical Systems B.V.) with 5-13 MHz linear probe. The patient was positioned in the supine position with the neck fully exposed. A total of two radiologists possessing 15 years of experience in thyroid US imaging evaluated the following sonographic features in consensus: Tumor location, size, orientation, margin, internal composition, echogenicity, microcalcification and blood flow signal. Representative US features are presented in Fig. 2. Any disagreements between the two radiologists were resolved by a third radiologist with 25 years of experience in thyroid sonography.

BRAF V600E mutation testing. BRAF V600E mutation testing was performed and the results were reviewed by experienced technicians in the clinical laboratory of Ruijin Hospital. Genomic DNA was extracted from the thyroid tissue samples using QIAamp® DNA Micro Kit (Qiagen, Inc.; cat. no. 56304) according to the instructions. The extracted DNA was subjected to PCR amplification (reagents: Ampli Taq Gold™ 360 Premix of Applied Biosystems; Thermo Fisher Scientific, Inc.; thermocycling conditions: 95˚C for 3 min, 95˚C 15 sec, 58˚C 30 sec, 72˚C 1 min, 72˚C 7 min, 35 cycles in total) and Sanger sequencing, and the sequencing data were interpreted using the low-frequency mutation analysis software Minor Variant Finder of Applied Biosystems (version 1.1; Thermo Fisher Scientific, Inc.). The sequencing primers used for BRAF V600E mutation testing are provided in Fig. S1. Sequencing traces for Sanger sequencing are shown in Fig. S2.

Contrast-enhanced CT assessment. All patients underwent scanning using multidetector CT scanners (GE Discovery CT750 HD 64 Slice CT Scanner, Cytiva; uCT 760; Shanghai United Imaging Healthcare Co., Ltd; and Philips Brilliance iCT 256, Philips Medical Systems B.V.) to collect CT data. All patients provided written informed consent and underwent iodine allergy testing before the examination. The slice thickness was 3.0 or 2.5 mm. Contrast-enhanced scans were performed at 45-65 sec after intravenous injection of non-ionic iodine contrast agent (2.5 m/s). The scanning range was scanned from C7 up to the base of the posterior fossa. The

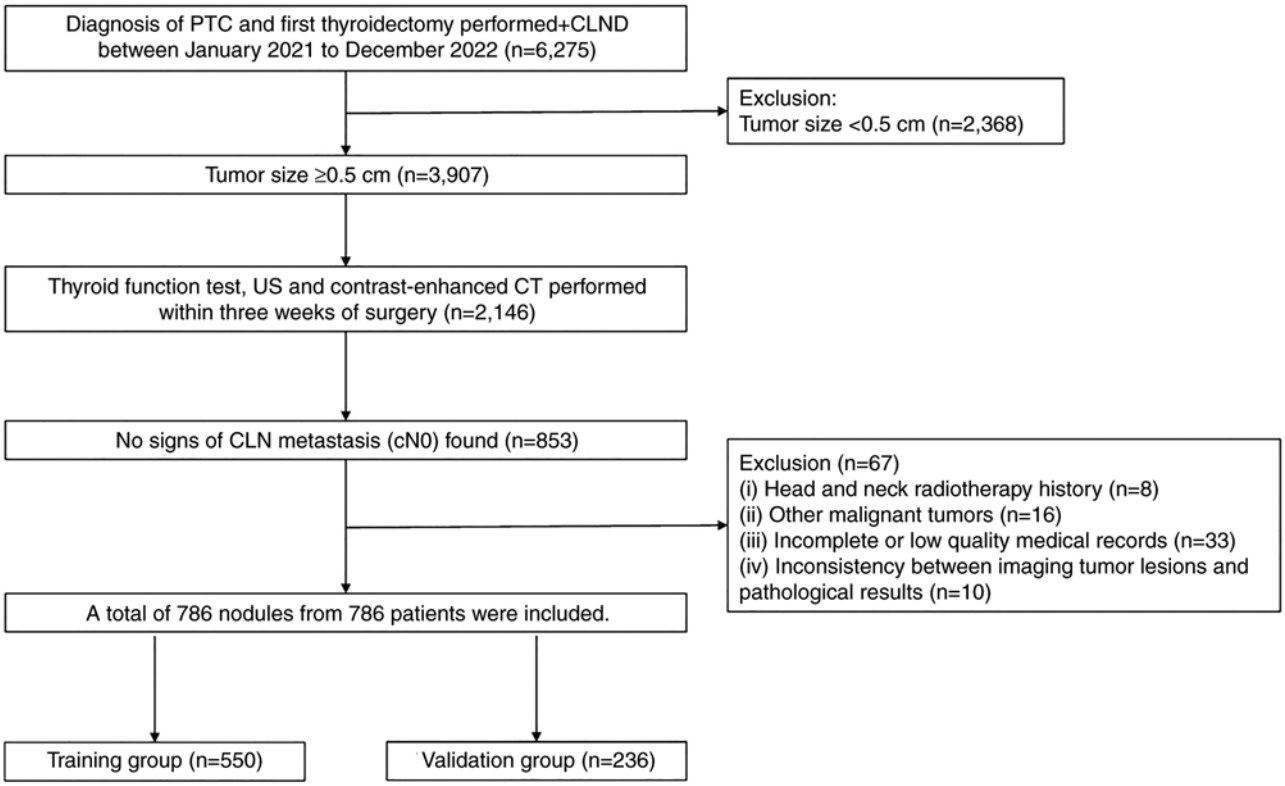

Figure 1. Flowchart of the present study. PTC, papillary thyroid cancer; CLND, central lymph node dissection; US, ultrasound; CT, computed tomography; cN0, clinically negative.

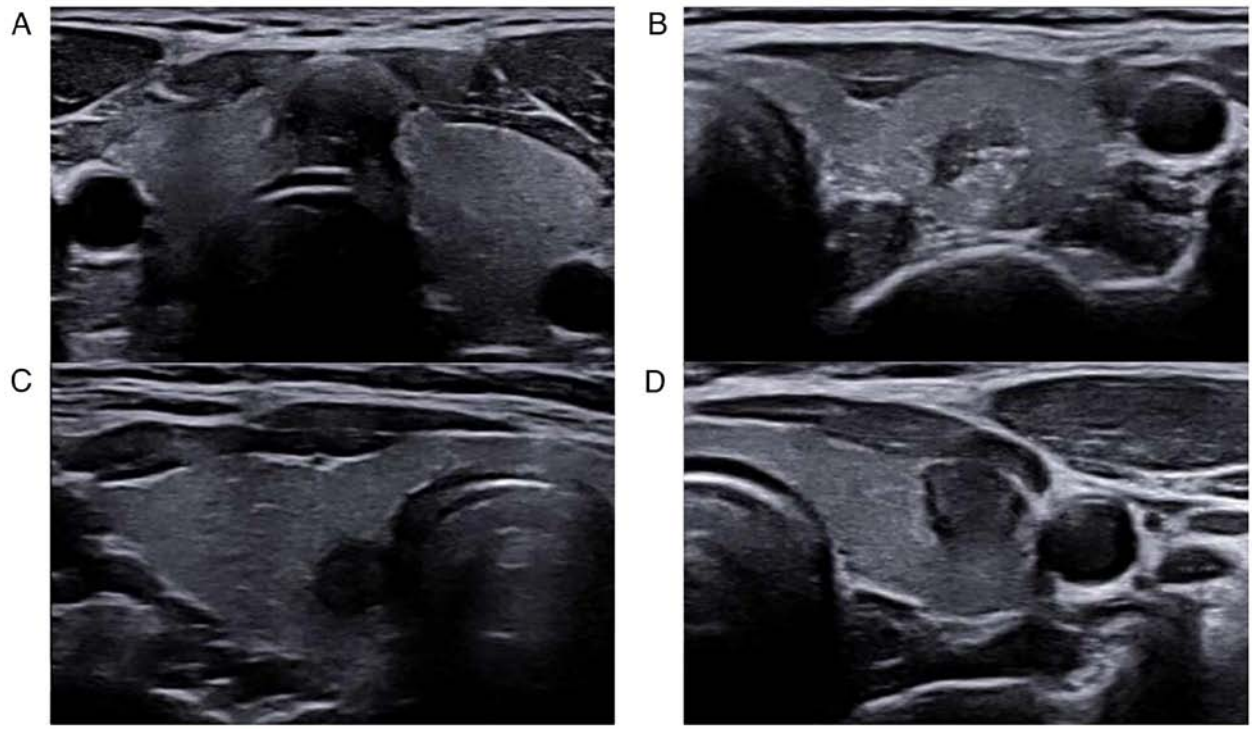

Figure 2. Representative ultrasound images. (A) Tumor location (isthmus). (B) Microcalcification. (C) Echogenicity (markedly hypoechoic). (D) Capsule contact.

CT findings of the following nodules were evaluated by two radiologists with extensive experience in thyroid CT imaging: i) Mean CT values of the lesions in the plain phase (UCT) and the venous phase (VCT). A circular region of interest was drawn at the maximum diameter of the lesion, excluding calcification, cystic components and artifacts, with the goal

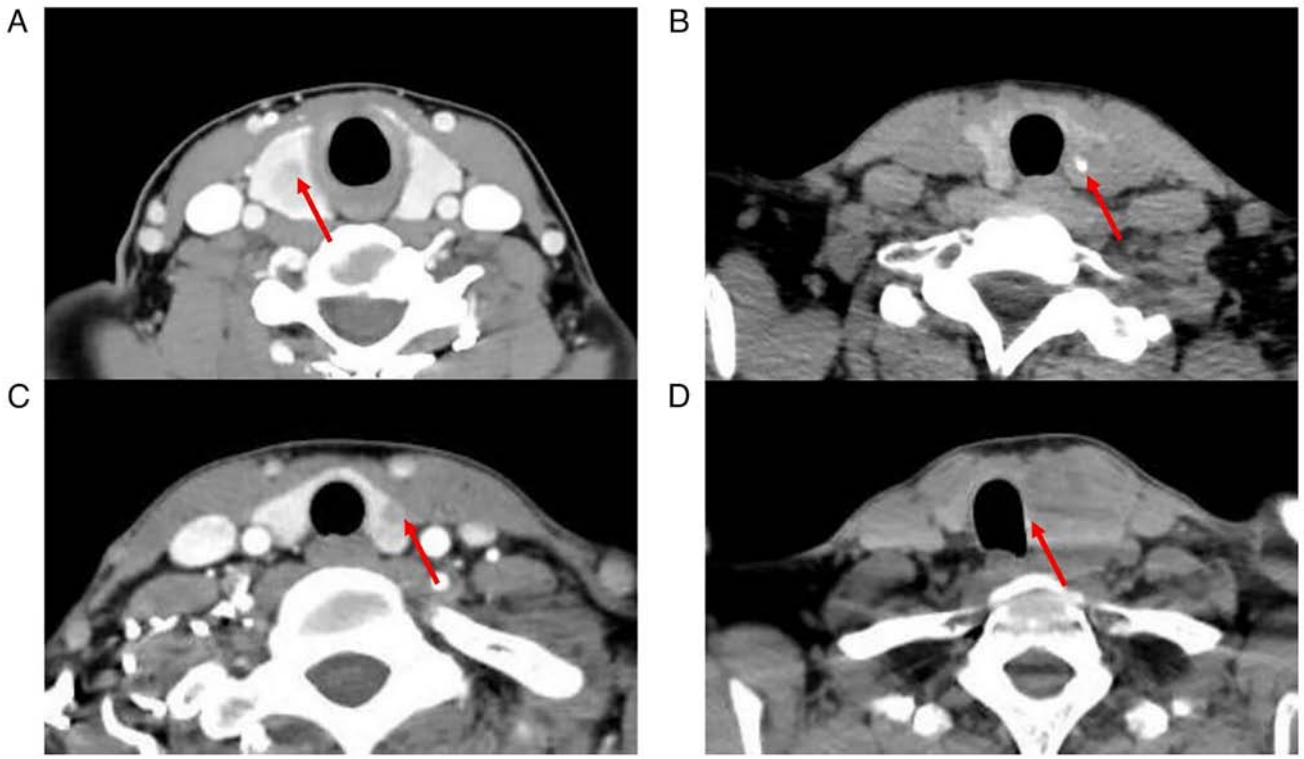

Figure 3. Representative contrast-enhanced computed tomography images. (A) Inhomogeneous enhancement (red arrow). (B) Calcification (red arrow). (C) Capsule invasion (red arrow). (D) Tracheal deviation (red arrow).

of covering >80% of the whole lesion area. ΔCT=VCT-UCT was used to evaluate the absolute enhanced CT value. The average value of two radiologists was used for further analysis; ii) homogeneity of enhancement was divided into homogeneity and inhomogeneity (Fig. 3A); iii) calcification (Fig. 3B); iv) capsule invasion (Fig. 3C); and v) tracheal deviation (Fig. 3D).

Variable definition and evaluation. Data for the following characteristics were collected to construct a retrospective database: i) Basic features: Age (45 years old as the cut point in accordance with the 7th Union for International Cancer Control/American Joint Committee on Cancer tumor-node-metastasis staging system) (24), sex (male/female), body mass index [BMI; 20.92 kg/m^2 as the cut point according to receiver operating characteristic (ROC) curve analysis], Hashimoto thyroiditis (HT; yes/no), BRAF V600E mutation (yes/no), TSH (reference, 0.35-4.94 μIU/ml), TG (reference, 3.5-77 ng/ml), TGAb (reference, <4.11) IU/ml) and TPOAb (reference, <5.61 IU/ml); ii) conventional US features: Tumor location (isthmus/non-isthmus), tumor number (unifocal/multifocal), tumor size (papillary thyroid microcarcinoma ≤1.0 cm and PTC >1.0 cm), tumor orientation (taller-than-wide/wider-than-tall), tumor margin (regular/irregular), internal composition (solid/non-solid), echogenicity (markedly hypoechoic/hypoechoic/isoechoic), capsule contact (yes/no; defined as thyroid nodule touching the thyroid boundary with or without capsule uplift), microcalcification (yes/no) and blood flow signal (poor/rich)' and iii) contrast-enhanced CT features: UCT, VCT, ΔCT, homogeneity of enhancement (homogeneity/inhomogeneity; defined as the degree of homogeneity of enhancement within the thyroid nodule), calcification (yes/no), capsule invasion (yes/no; defined as the maximum diameter of the nodule was located at the junction of the nodule and thyroid gland or at the lateral side of the thyroid gland, known as 'cookie bite sign') and tracheal deviation (yes/no). ROC curve analysis revealed that the UCT value was 65.35 Hu, the VCT value was 183.90 Hu, and ΔCT was 111.50 Hu as the cut-off point of CLNM in the population of the present study (data not presented).

Statistical analysis. Continuous data were transformed into categorical data using cut-off values established through ROC curve analysis for enhanced clinical comprehension. Data are presented as the frequency or mean ± standard deviation. UCT, VCT and ΔCT were analyzed using an independent samples t-test, and TSH and echogenicity were analyzed using Fisher's exact test. All other variables were analyzed using the χ^2 test. Multivariate logistic regression analysis was used to determine independent factors. Based on the results of multivariate logistic regression analysis, a nomogram for predicting CLNM was developed and evaluated using ROC curves, calibration curves and decision curve analysis (DCA) curves. All statistical analyses were performed using SPSS version 27.0 (IBM Corp.) and R version 4.3.2 (The R Foundation) software. P<0.05 was considered to indicate a statistically significant difference.

Results

Characteristics of patients. Patients were divided into the training group (n=550) and validation group (n=236). CLNM occurred in 39.1% (215/550) of the patients in the training

Table I. Characteristics of all patients in the training and validation group.

A, Clinical characteristics

Characteristic	Training group (n=550)	Validation group (n=236)	P-value
Age (%)			0.620
≤45 years	401 (72.91)	168 (71.19)	
>45 years	149 (27.09)	68 (28.81)	
Sex (%)			0.399
Male	138 (25.09)	66 (27.97)	
Female	412 (74.91)	170 (72.03)	
BMI, kg/m^2	23.74±3.57	23.59±3.59	0.596
With HT (%)			0.150
Yes	100 (18.18)	33 (13.98)	
No	450 (81.82)	203 (86.02)	
BRAF V600E mutation (%)			0.863
Yes	448 (81.45)	191 (80.93)	
No	102 (18.55)	45 (19.07)	
TSH (%)			0.191
Low	9 (1.64)	3 (1.27)	
Normal	536 (97.45)	227 (96.19)	
High	5 (0.91)	6 (2.54)	
TG (%)			0.105
Low	95 (17.27)	29 (12.29)	
Normal	425 (77.27)	188 (79.66)	
High	30 (5.45)	19 (8.05)	
TGAb (%)			0.125
Negative	351 (63.82)	164 (69.49)	
Positive	199 (36.18)	72 (30.51)	
TPOAb (%)			0.658
Negative	428 (77.82)	187 (79.24)	
Positive	122 (22.18)	49 (20.76)	

B, US characteristics

Characteristic	Training group (n=550)	Validation group (n=236)	P-value
Tumor location (%)			0.682
Isthmus	22 (4.00)	8 (3.39)	
Non-isthmus	528 (96.00)	228 (96.61)	
Tumor number (%)			0.472
Unifocal	412 (74.91)	171 (72.46)	
Multifocal	138 (25.09)	65 (27.54)	
Tumor size (%)			0.589
≤1.0 mm	395 (71.82)	165 (69.92)	
>1.0 mm	155 (28.18)	71 (30.08)	
Tumor shape (%)			0.768
Taller-than-wide	278 (50.55)	122 (51.69)	
Wider-than-tall	272 (49.45)	114 (48.31)	
Margin (%)			0.500
Irregular	511 (92.91)	216 (91.53)	
Regular	39 (7.09)	20 (8.47)	
Composition (%)			0.943
Solid	525 (95.45)	225 (95.34)	
Non-solid	25 (4.55)	11 (4.66)	

Table I. Continued.

B, US characteristics

Characteristic	Training group (n=550)	Validation group (n=236)	P-value
Echogenicity (%)			0.140
Markedly hypoechoic	19 (3.45)	8 (3.39)	
Hypoechoic	527 (95.82)	222 (94.07)	
Isoechoic	4 (0.73)	6 (2.54)	
Capsule contact (%)			0.557
Yes	405 (73.64)	169 (71.61)	
No	145 (26.36)	67 (28.39)	
Microcalcification (%)			0.238
Yes	407 (74.00)	184 (77.97)	
No	143 (26.00)	52 (22.03)	
Blood flow signal (%)			0.159
Rich	89 (16.18)	48 (20.34)	
poor	461 (83.82)	188 (79.66)	

C, CT characteristics

Characteristic	Training group (n=550)	Validation group (n=236)	P-value
UCT, Hu	61.11±17.51	62.92±16.84	0.174
VCT, Hu	130.69±35.10	131.64±34.84	0.726
ΔCT, Hu	69.58±28.95	67.72±29.71	0.419
Homogeneity of enhancement (%)			0.219
Inhomogeneity	488 (88.73)	202 (85.59)	
Homogeneity	62 (11.27)	34 (14.41)	
Calcification (%)			0.091
Yes	91 (16.55)	51 (21.61)	
No	459 (83.45)	185 (78.39)	
Capsule invasion (%)			0.382
Yes	254 (46.18)	117(49.58)	
No	296 (53.82)	119 (50.42)	
Tracheal deviation (%)			0.852
Yes	15 (2.73)	7 (2.97)	
No	535 (97.27)	229 (97.03)	

UCT, mean CT values in plain phase; VCT, mean CT values in venous phase; ΔCT=VCT-UCT. Data are presented as n or mean ± standard deviation. UCT, VCT and ΔCT were analyzed using the t test, TSH and echogenicity were analyzed using Fisher's exact test, and all other variables were analyzed using the χ^2 test. BMI, body mass index; HT, Hashimoto thyroiditis; TSH, thyroid stimulating hormone; TG, thyroglobulin; TGAb, TG antibody; TPOAb, thyroid peroxidase antibody; US, ultrasound; CT, computed tomography.

group and 38.6% (91/236) of the patients in the validation group. In total, 38.9% of patients (306/786) had an CLNM(-) status before surgery, but had confirmed CLNM using postoperative pathology. As demonstrated in Table I, there was no significant difference between the two groups (P>0.05), which indicated their rationality as training and validation groups.

Univariate analysis of CLNM. In the univariate analysis, CLNM was significantly associated with a younger age (≤45 years; P<0.001), the male sex (P<0.001), no HT (P=0.001), negative TGAb (P=0.004) and negative TPOAb (P=0.002). However, there were no significant differences for BMI, presence of BRAF V600E mutation, level of TSH or level of TG.

Among the US features, tumor location (isthmus; P<0.001), tumor size (>1.0 cm; P<0.001), presence of microcalcification (P<0.001) and capsule contact (yes; P<0.001) were significantly different between CLNM and non-CLNM groups. However, there was no significant difference for tumor number, tumor shape, tumor margin, internal composition, echogenicity or blood flow signal.

Table II. Univariate analysis of characteristics in the training group.

A, Clinical characteristics

Characteristic	CLNM(+) group (n=215)	CLNM(-) group (n=335)	P-value
Age (%)			<0.001[a]
≤45 years	174 (80.93)	227 (67.76)	
>45 years	41 (19.07)	108 (32.24)	
Sex (%)			<0.001[a]
Male	77 (35.81)	61 (18.21)	
Female	138 (64.19)	274 (81.79)	
BMI (%)			0.168
≤20.92 kg/m^2	43 (20.00)	84 (25.07)	
>20.92 kg/m^2	172 (80.00)	251(74.93)	
With HT (%)			0.001[a]
Yes	25 (11.63)	75 (22.39)	
No	190 (88.37)	260 (77.61)	
BRAF V600E mutation (%)			0.187
Yes	181 (84.19)	267 (79.70)	
No	34 (15.81)	68 (20.30)	
TSH (%)			0.757
Low	3 (1.40)	6 (1.79)	
Normal	211 (98.14)	325 (97.01)	
High	1 (0.47)	4 (1.19)	
TG (%)			0.107
Low	28 (13.02)	67 (20.00)	
Normal	175 (81.40)	250 (74.63)	
High	12 (5.58)	18 (5.37)	
TGAb (%)			0.004[a]
Negative	153 (71.16)	198 (59.10)	
Positive	62 (28.84)	137 (40.90)	
TPOAb (%)			0.002[a]
Negative	182 (84.65)	246 (73.43)	
Positive	33 (15.35)	89 (26.57)	

B, US characteristics

Characteristic	CLNM(+) group (n=215)	CLNM(-) group (n=335)	P-value
Tumor location (%)			<0.001[a]
Isthmus	16 (7.44)	6 (1.79)	
Non-isthmus	199 (92.56)	329 (98.21)	
Tumor number (%)			0.538
Unifocal	158 (73.49)	254 (75.82)	
Multifocal	57 (26.51)	81 (24.18)	
Tumor size (%)			<0.001[a]
≤1.0 mm	128 (59.53)	267 (79.70)	
>1.0 mm	87 (40.47)	68 (20.30)	
Tumor shape (%)			0.414
Taller-than-wide	104 (48.37)	174 (51.94)	
Wider-than-tall	111 (51.63)	161 (48.06)	
Margin (%)			0.148
Irregular	204 (94.88)	307 (91.64)	
Regular	11 (5.12)	28 (8.36)	

Table II. Continued.

B, US characteristics

Characteristic	CLNM(+) group (n=215)	CLNM(-) group (n=335)	P-value
Composition (%)			0.457
Solid	207 (96.28)	318 (94.93)	
Non-solid	8 (3.72)	17 (5.07)	
Echogenicity (%)			0.263
Markedly hypoechoic	4 (1.86)	15 (4.48)	
Hypoechoic	209 (97.21)	318 (94.93)	
Isoechoic	2 (0.93)	2 (0.60)	
Capsule contact (%)			<0.001[a]
Yes	179 (83.26)	226 (67.46)	
No	36 (16.74)	109 (32.54)	
Microcalcification (%)			<0.001[a]
Yes	178 (82.79)	229 (68.36)	
No	37 (17.21)	106 (31.64)	
Blood flow signal (%)			0.508
Rich	32 (14.88)	57 (17.01)	
Poor	183 (85.12)	278 (82.99)	

C, CT characteristics

Characteristics	CLNM(+) group (n=215)	CLNM(-) group (n=335)	P-value
UCT (%)			0.155
≤65.35 Hu	135 (62.79)	230 (68.66)	
>65.35 Hu	80 (37.21)	105 (31.34)	
VCT (%)			0.208
≤183.90 Hu	200 (93.02)	320 (95.52)	
>183.90 Hu	15 (6.98)	15 (4.48)	
ΔCT (%)			0.173
≤111.50 Hu	194 (90.23)	313 (93.43)	
>111.50 Hu	21 (9.77)	22 (6.57)	
Homogeneity of enhancement (%)			0.002[a]
Inhomogeneity	202 (93.95)	286 (85.37)	
Homogeneity	13 (6.05)	49 (14.63)	
Calcification (%)			0.007[a]
Yes	47 (21.86)	44 (13.13)	
No	168 (78.14)	291 (86.87)	
Capsule invasion (%)			<0.001[a]
Yes	155 (72.09)	99 (29.55)	
No	60 (27.91)	236 (70.45)	
Tracheal deviation (%)			0.643
Yes	5 (2.33)	10 (2.99)	
No	210 (97.67)	325 (97.01)	

UCT, mean CT values in plain phase; VCT, mean CT values in venous phase; ΔCT=VCT-UCT. [a]P<0.05. BMI, body mass index; HT, Hashimoto thyroiditis; TSH, thyroid stimulating hormone; TG, thyroglobulin; TGAb, TG antibody; TPOAb, thyroid peroxidase antibody; US, ultrasound; CT, computed tomography; CLNM, central lymph node metastasis.

In terms of contrast-enhanced CT characteristics, there were significant differences for an inhomogeneous enhancement (P=0.002), presence of calcification (P=0.007) and capsule invasion (P<0.001), but there were no significant

Table III. Multivariate analysis of characteristics in the training group.

Variable	B coefficient	OR	95% CI	P-value
Age				
≤45 years	-0.037	0.964	0.945-0.982	<0.001[a]
>45 years				
Sex				
Male	0.764	2.147	1.332-3.459	0.002[a]
Female				
With HT				
Yes	0.922	2.515	1.208-5.239	0.014[a]
No				
TGAb				
Negative	0.196	1.216	0.681-2.173	0.509
Positive				
TPOAb				
Negative	-0.629	0.533	0.277-1.025	0.059
Positive				
US-tumor location				
Isthmus	-1.554	0.211	0.067-0.669	0.008[a]
Non-isthmus				
US-tumor size				
≤1.0 mm	-0.264	0.768	0.466-1.265	0.300
>1.0 mm				
US-capsule contact				
Yes	-0.418	0.659	0.399-1.088	0.103
No				
US-microcalcification				
Yes	-0.529	0.589	0.355-0.979	0.041[a]
No				
CT-homogeneity of enhancement				
Inhomogeneity	0.997	2.711	1.268-5.798	0.010[a]
Homogeneity				
CT-capsule invasion				
Yes	1.866	6.463	4.103-10.181	<0.001[a]
No				
CT-calcification				
Yes	-0.450	0.638	0.368-1.106	0.110
No				

[a]P<0.05. HT, Hashimoto thyroiditis; TSH, thyroid stimulating hormone; TGAb, TG antibody; TPOAb, thyroid peroxidase antibody; US, ultrasound; CT, computed tomography; OR, odds ratio; CI, confidence interval.

differences for UCT, VCT, ΔCT or tracheal deviation between the two groups (Table II).

Multivariate logistic regression analysis of CLNM. The characteristics with statistical significance identified in the univariate analysis were further analyzed using multivariate logistic regression analysis. The results demonstrated that the following predictors were significantly independently associated with promoting CLNM in patients with PTC: Age of ≤45 years old [odds ratio (OR)=0.964; 95% confidence interval (CI), 0.945-0.982; P<0.001], male sex (OR=2.147; 95% CI, 1.332-3.459; P=0.002), no HT (OR=2.515; 95% CI, 1.208-5.239; P=0.014), isthmic tumor (OR=0.211; 95% CI, 0.067-0.669; P=0.008), presence of microcalcification (OR=0.589; 95% CI, 0.355-0.979; P=0.041), inhomogeneous enhancement (OR=2.711; 95% CI, 0.355-0.979; P=0.041). 95%CI 1.268-5.798, P=0.010) and capsule invasion (OR=6.463; 95% CI, 4.103-10.181; P<0.001; Table III).

Development and validation of the individualized prediction nomogram. According to the results of multivariate logistic

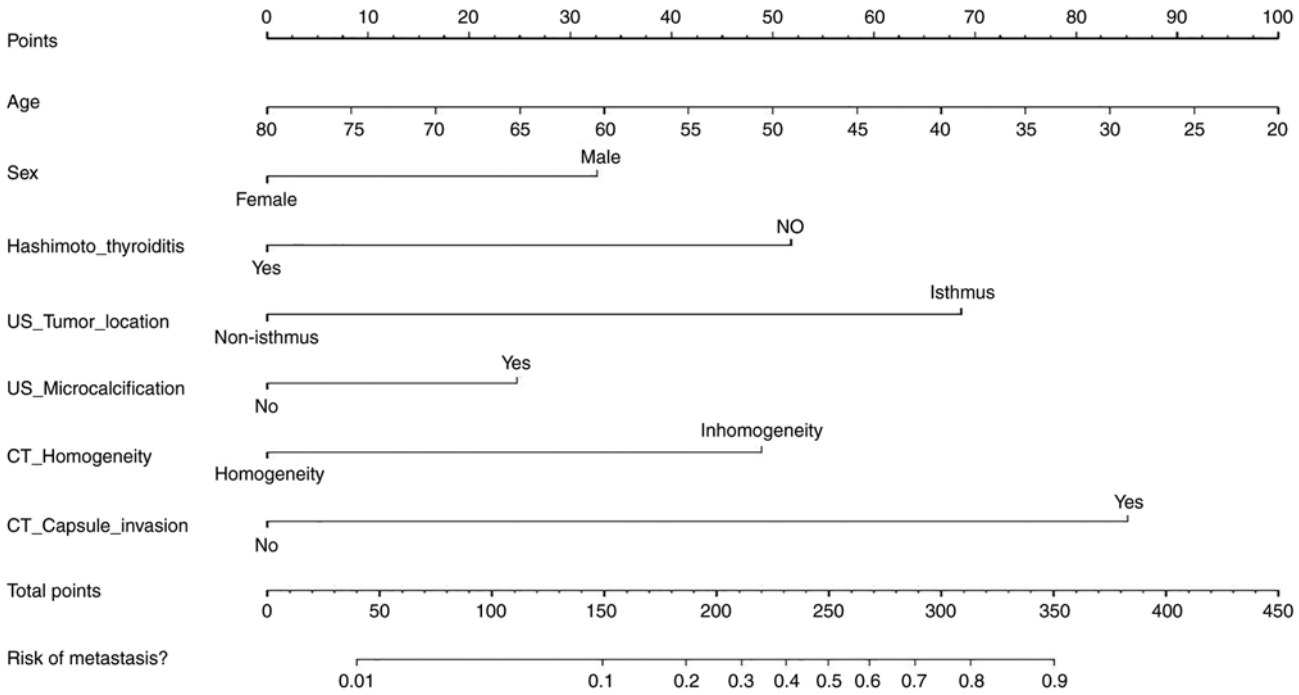

Figure 4. Nomogram for predicting central lymph node metastasis. US, ultrasound; CT, computed tomography.

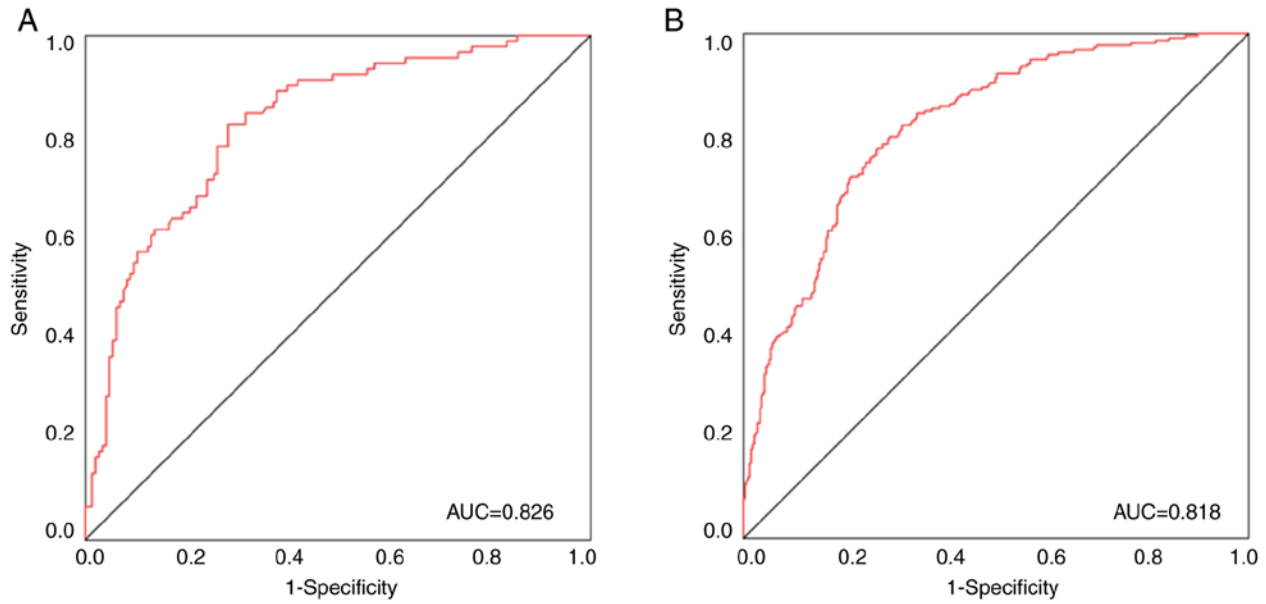

Figure 5. Receiver operating characteristic curves. (A) Training group. (B) Validation group. AUC, area under the curve.

regression analysis, 7 variables including age, sex, presence of HT, tumor location, microcalcification, homogeneity of enhancement and capsule invasion were used in the development of a personalized prediction nomogram for predicting CLNM in patients with PTC (Fig. 4). According to the ROC curve, the area under the curve (AUC) was 0.826, the sensitivity was 0.824 and the specificity was 0.717 for the training group, whilst the AUC was 0.818, the sensitivity was 0.725 and the specificity was 0.781 for the validation group (Fig. 5A and B). In addition, the AUC for predicting CLNM without combined contrast-enhanced CT was 0.712, and the AUC of predicting CLNM increased to 0.818 when clinical and conventional US and contrast-enhanced CT features were combined (Fig. 6). This further demonstrates the advantage of the US combined CT model.

Furthermore, calibration curves depicting the CLNM risk nomogram in patients with PTC were generated to assess the effectiveness of the nomogram. The curves indicated a satisfactory agreement in both the training and validation groups, with mean absolute errors of 0.021 (Fig. 7A) and 0.023 (Fig. 7B), respectively.

Clinical application. Finally, DCA was performed to evaluate the performance of the model in detecting CLNM for patients

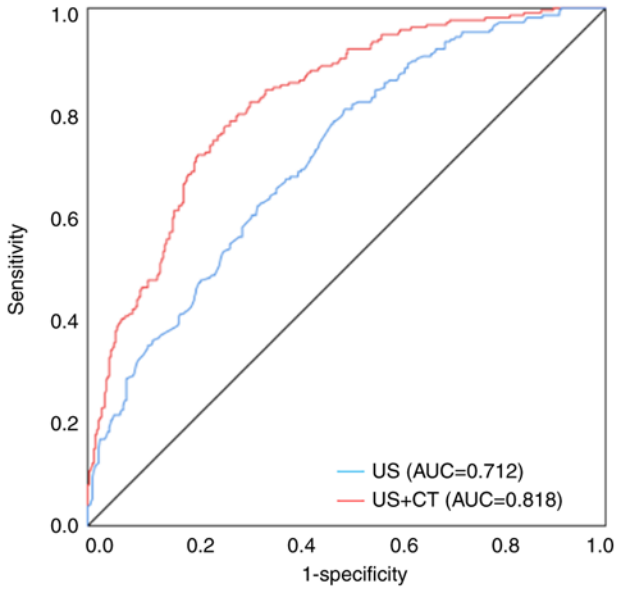

Figure 6. ROC curves. The area under the ROC curve for predicting central lymph node metastasis based on clinical, US and contrast-enhanced CT features was higher than that of not combining contrast-enhanced CT features. ROC, receiver operating characteristic; US, ultrasound; CT, computed tomography; AUC, area under the curve.

with PTC (Fig. 8). The DCA curve demonstrated that it would be beneficial to predict CLNM with the nomogram when the threshold probability ranges from 0.1 to 1.0.

Discussion

Most PTCs show a slow and indolent growth pattern, and the overall prognosis is favorable, with a current 5-year survival rate of >90% (25). CLNM is occurs in 12-64% of patients with PTC, and exhibits a strong association with increased recurrence and poor overall survival (26). Therefore, precise preoperative prediction of CLNM can be advantageous for patients with PTC (cN0), and creating an effective prediction model would serve as a viable solution. Previous studies have reported that US features of PTC can help predict CLNM in patients, but few of them mentioned the role of CT in this (27-29). In the present study, the US and CT features of patients with PTC were reviewed and the value of US combined with contrast-enhanced CT for predicting CLNM was evaluated.

Many studies have reported that sex and age are independent risk factors for CLNM in PTC, among which the male sex and a younger age (≤45 years) have a greater risk of CLNM (30-32). This is consistent with the findings obtained in the present study. However, the multifocality and tumor size characteristics did not differ significantly between the two groups in the present study, which is not consistent with previous studies (22,31,33). The potential reasons contributing to this variation may be the different sample sizes and evaluation criteria used for characteristics.

HT is the most common autoimmune thyroid disease and 10-58% of patients with PTC have it (34). In most studies, HT has been regarded as a protective factor for CLNM in PTC (35,36), and Jara *et al* (37) also noted that HT correlated with less aggressive disease and a reduced incidence of lymph node metastasis. Moreover, the present study also demonstrated that patients with PTC but without coexistent HT were more prone to CLNM. However, Mao *et al* (38) and Liu *et al* (39) suggested that HT had no significant effect on the incidence of lymph node metastasis. Therefore, the effect of HT on CLNM in PTC is uncertain, and more clinical trials emphasizing the influence of HT on the progression of PTC are worth performing.

To the best of our knowledge, the relationship between PTC tumor location and lymph node metastasis is controversial. Certain studies reported that there is no significant association between tumor location and CLNM (22,40). However, Li *et al* (41) and Lyu *et al* (42) suggested that isthmic tumors are more prone to CLNM compared with lateral lobe tumors. The present study also demonstrated that tumor location in the isthmus was significantly associated with CLNM. The thyroid isthmus is typically situated anteriorly to the cartilaginous ring of the second to fourth trachea, where the gland thins to a thickness of only ~2 mm. Due to the specific location of the tumor, the isthmus tumor is adjacent to the trachea and thyroid capsule, so the incidence of extrathyroidal extension, CLNM and multifocality is higher than that of thyroid lobe tumor (43). In addition, the lymphatic drainage pattern of the thyroid isthmus differs from that of the thyroid lobe (41). The presence of the aforementioned features will increase the risk of CLNM in in isthmic tumors (42). Notably, although patients with isthmic tumors were demonstrated to have a higher risk of CLNM, the incidence of this feature was low, accounting for only 4.0% (22/550) of the total cases in the present study.

US is known to provide a better soft tissue resolution than CT, and microcalcifications seen by US are not necessarily shown on CT (44,45). Therefore, in the present study, microcalcifications were evaluated by US, whilst calcifications evaluated by CT were generally macrocalcifications. The present study confirmed that the presence of microcalcification was an independent predictor of CLNM in cN0 PTC and that macrocalcification was not significantly associated with CLNM. Previous studies have also reported an association between microcalcification and CLNM in PTC (46-48). Microcalcifications are characterized as punctate bright echoes with or without accompanying acoustic shadowing, mainly small psammoma bodies of 10-100 μm, arranged in concentric layers (49). Therefore, as microcalcification may be a predictive marker for CLNM (50), when microcalcification is found in thyroid nodules by preoperative examination, a more meticulous evaluation of the central cervical lymph nodes is warranted.

Angiogenesis is known to be associated with aggressive tumor growth and metastasis (51). Contrast-enhanced CT provides improved visualization of the tumor microvascular distribution (33). There were a large number of neovascularization in the thyroid tumor tissue, which appeared to be enhanced after enhancement. However, at the same time, this malignant growth will destroy a lot of tissue structures and blood vessels, so the degree of enhancement is lower than that of normal thyroid (52). Furthermore, heterogeneous vascular distribution can lead to inhomogeneous enhancement shown on contrast-enhanced CT images. The present study demonstrated that although the incidence of inhomogeneous

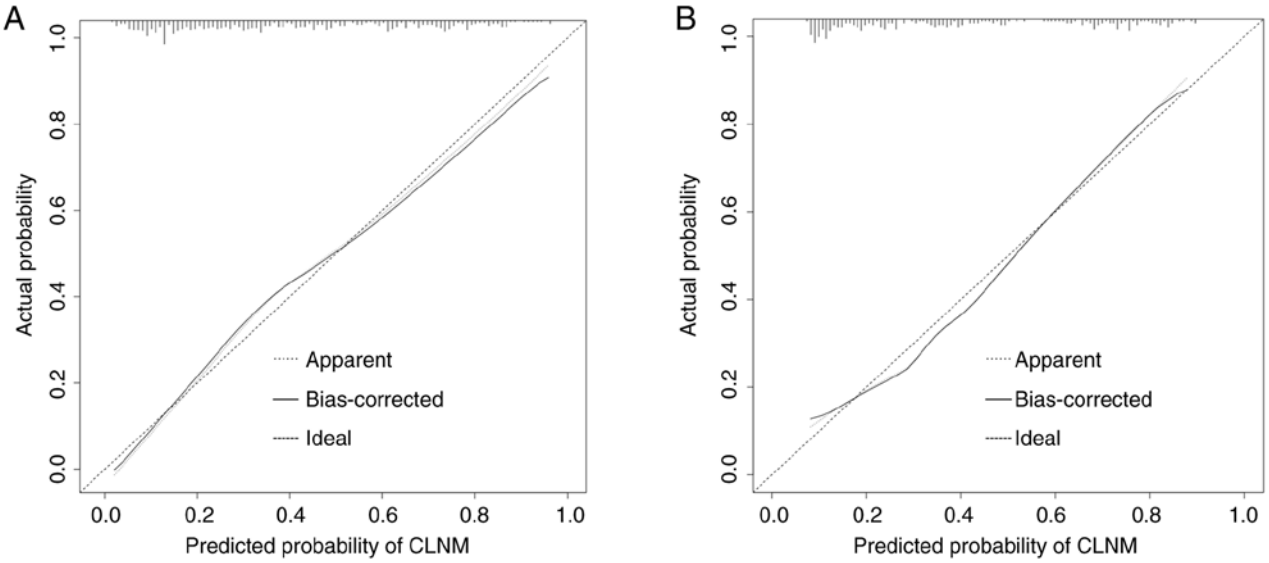

Figure 7. Calibration curves. (A) Training group. (B) Validation group. CLNM, central lymph node metastasis.

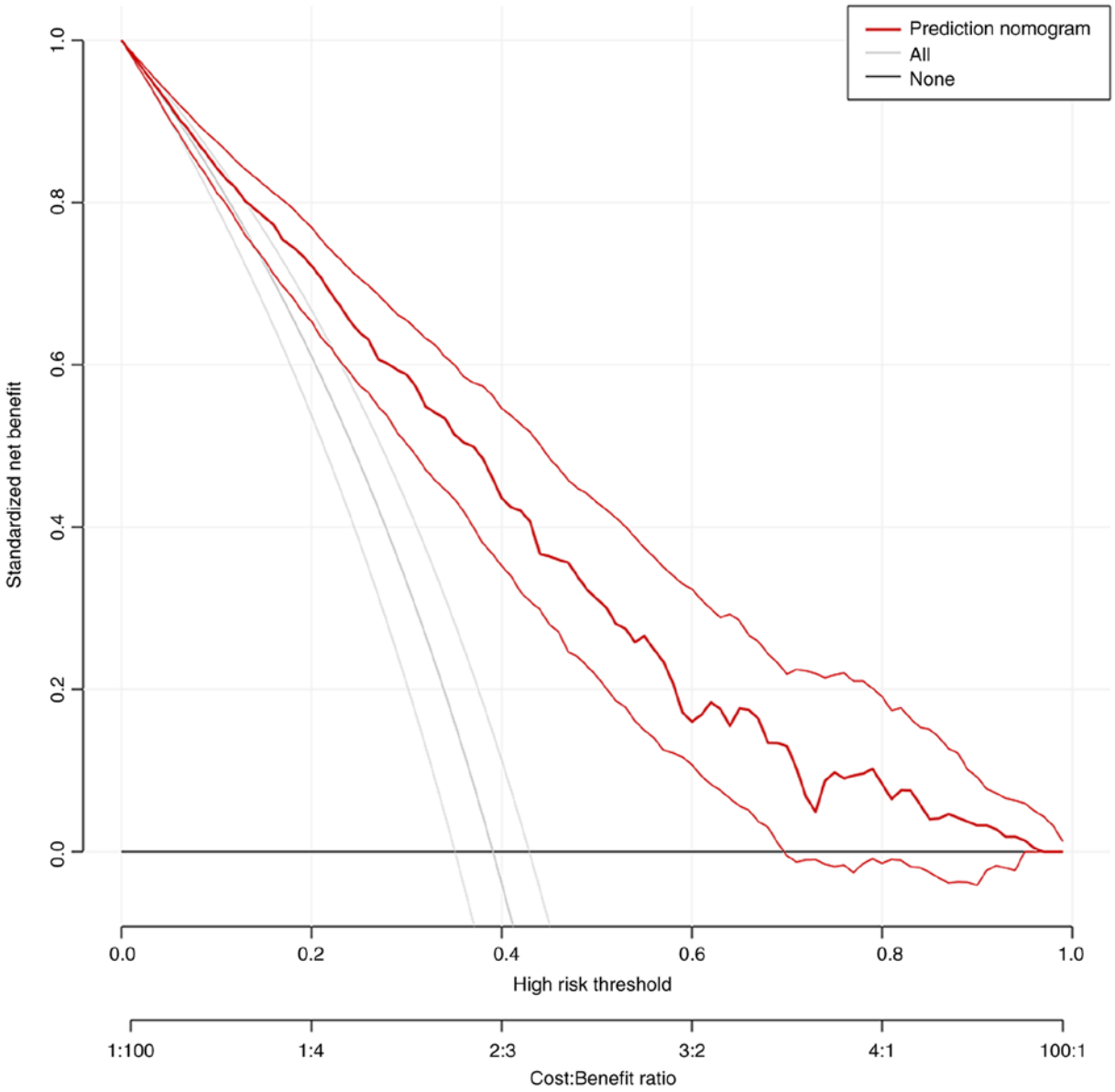

Figure 8. Decision curve analysis for the nomogram.

enhancement was relatively high, it was also significantly associated with predicting CLNM.

Capsule invasion is generally regarded as being associated with CLNM. However, whether US or contrast-enhanced CT is superior in predicting capsule invasion is still controversial (19). Yang *et al* (23) reported that observation of the anterior thyroid capsule by US is influenced by US near-field artifacts, whilst observation of the lateral and posterior thyroid capsules is hindered by the presence of blood vessels and the trachea, which may not be distinctly depicted (8). In addition, considering the strong dependence of US on the operator (15), the present study included capsule contact on US images and capsule invasion on CT images, which were associated but not consistent. The present study demonstrated that capsule invasion assessed by CT is an independent risk factor for CLNM, and its mechanism may be linked to the abundant thyroid lymphatic network. If the tumor breaks through the capsule, it has the potential to readily induce lymph node metastasis in the central region (8,53).

Few studies have investigated the relationship between contrast-enhanced CT features and CLNM. For example, Peng *et al* (54) and Mou *et al* (55) collected data from preoperative CT images to predict CLNM in patients with cN0 PTC, but the studies only had small sample sizes. Moreover, Zhao *et al* (33) used a simple risk-scoring system to predict CLNM. To the best of our knowledge, the present study was the first with an adequate sample size to construct a nomogram combining US with contrast-enhanced CT for predicting CLNM.

Nonetheless, there were several limitations of the present study that should be acknowledged. First, the study design was retrospective, making it susceptible to inherent bias in patient recruitment and data collection. Second, the retrospective nature of the present study may limit the analysis of additional potential variables. Analyses were performed only on the basis of the characteristics of the primary tumor. Furthermore, the present study lacks external validation. Therefore, it is imperative to prioritize additional external validation cohorts from prospective studies to comprehensively assess the viability of the nomogram in the present study. In addition, for multifocal tumors, analysis was performed only on the largest tumor, and the features of the remaining tumors were unknown. Notably, the present study did not assess patients with PTCs that were <0.5 cm.

Despite the limitations, the present study presents certain highlights. Based on the aforementioned clinical, US and contrast-enhanced CT characteristics, the present study developed and validated a novel nomogram, which has an improved diagnostic performance in predicting CLNM than no combination of contrast-enhanced CT. Moreover, the nomogram serves as a user-friendly diagnostic tool for predicting CLNM. By adding the specific scores of each predictor, the corresponding CLNM probability for thyroid nodules can be obtained. Overall, this prediction model could make it possible to personalize the CLNM prediction of most patients with PTC and help surgeons make decisions on surgical options to maximize the benefits of patients.

In conclusion, the findings of the present study suggest that a young age, the male sex, no presence of HT, isthmic tumor, microcalcification, inhomogeneous enhancement and capsule invasion are significantly associated with CLNM in patients with cN0 PTC. Furthermore, the constructed nomogram has the potential to be used for preoperative risk assessment of CLNM, which can help surgeons better develop appropriate surgical plans, providing a novel approach to managing patients with cN0 PTC.

Acknowledgements

Not applicable.

Funding

No funding was received.

Availability of data and materials

The data generated in the present study may be requested from the corresponding author.

Authors' contributions

QZ, SX, JY and WZ conceived and designed the study. QZ, SX, QS and YM contributed to data collection and data analyses. QZ and SX, YH and YM performed the data interpretation. QZ, SX, YH and YM contributed to the statistical analysis. QZ, SX, YH and YM drafted the manuscript. QS, JY and WZ revised the manuscript critically for important intellectual content. QS, JY and WZ confirm the authenticity of all the raw data. QZ, SX, QS, YM, YH, JY and WZ discussed the results and contributed to the revision of the final manuscript. All authors read and approved the final version of the manuscript.

Ethics approval and consent to participate

The present study was approved by the Ethics Committee of Ruijin Hospital, Shanghai Jiao Tong University School of Medicine (Shanghai, China; approval no. 2023-129). The requirement for informed consent to participate was waived by the Ethics Committee as the present study is retrospective. All methods were performed in accordance with the Helsinki Declaration and local legislation and institutional requirements.

Patient consent for publication

Not applicable.

Competing interests

The authors declare that they have no competing interests.

References

1. Sung H, Ferlay J, Siegel RL, Laversanne M, Soerjomataram I, Jemal A and Bray F: Global cancer statistics 2020: GLOBOCAN estimates of incidence and mortality worldwide for 36 cancers in 185 countries. CA Cancer J Clin 71: 209-249, 2021.
2. Chen DW, Lang BHH, McLeod DSA, Newbold K and Haymart MR: Thyroid cancer. Lancet 401: 1531-1544, 2023.

3. Papaleontiou M, Evron JM, Esfandiari NH, Reyes-Gastelum D, Ward KC, Hamilton AS, Worden F and Haymart MR: Patient report of recurrent and persistent thyroid cancer. Thyroid 30: 1297-1305, 2020.
4. Dai Q, Liu D, Tao Y, Ding C, Li S, Zhao C, Wang Z, Tao Y, Tian J and Leng X: Nomograms based on preoperative multimodal ultrasound of papillary thyroid carcinoma for predicting central lymph node metastasis. Eur Radiol 32: 4596-4608, 2022.
5. Al Afif A, Williams BA, Rigby MH, Bullock MJ, Taylor SM, Trites J and Hart RD: Multifocal papillary thyroid cancer increases the risk of central lymph node metastasis. Thyroid 25: 1008-1012, 2015.
6. Heng Y, Yang Z, Lin J, Liu Q, Cai W and Tao L: Risks of central lymph node metastasis in papillary thyroid carcinoma with or without multifocality in at least one lobe: A multi-center analysis. Oral Oncol 134: 106185, 2022.
7. Haugen BR, Alexander EK, Bible KC, Doherty GM, Mandel SJ, Nikiforov YE, Pacini F, Randolph GW, Sawka AM, Schlumberger M, *et al*: 2015 American thyroid association management guidelines for adult patients with thyroid nodules and differentiated thyroid cancer: The American thyroid association guidelines task force on thyroid nodules and differentiated thyroid cancer. Thyroid 26: 1-133, 2016.
8. Guang Y, He W, Zhang W, Zhang H, Zhang Y and Wan F: Clinical study of ultrasonographic risk factors for central lymph node metastasis of papillary thyroid carcinoma. Front Endocrinol (Lausanne) 12: 791970, 2021.
9. Mazzaferri EL, Doherty GM and Steward DL: The pros and cons of prophylactic central compartment lymph node dissection for papillary thyroid carcinoma. Thyroid 19: 683-689, 2009.
10. Shaha AR: Central lymph node metastasis in papillary thyroid carcinoma. World J Surg 42: 630-631, 2018.
11. Xue J, Teng D and Wang H: Efficacy and safety of ultrasound-guided radiofrequency ablation for papillary thyroid microcarcinoma: A systematic review and meta-analysis. Int J Hyperthermia 39: 1300-1309, 2022.
12. Zhou J, Yin L, Wei X, Zhang S, Song Y, Luo B, Li J, Qian L, Cui L, Chen W, *et al*: 2020 Chinese guidelines for ultrasound malignancy risk stratification of thyroid nodules: The C-TIRADS. Endocrine 70: 256-279, 2020.
13. Alexander EK and Cibas ES: Diagnosis of thyroid nodules. Lancet Diabetes Endocrinol 10: 533-539, 2022.
14. Roh JL, Park JY, Kim JM and Song CJ: Use of preoperative ultrasonography as guidance for neck dissection in patients with papillary thyroid carcinoma. J Surg Oncol 99: 28-31, 2009.
15. Hwang HS and Orloff LA: Efficacy of preoperative neck ultrasound in the detection of cervical lymph node metastasis from thyroid cancer. Laryngoscope 121: 487-491, 2011.
16. Kim E, Park JS, Son KR, Kim JH, Jeon SJ and Na DG: Preoperative diagnosis of cervical metastatic lymph nodes in papillary thyroid carcinoma: Comparison of ultrasound, computed tomography, and combined ultrasound with computed tomography. Thyroid 18: 411-418, 2008.
17. Suh CH, Baek JH, Choi YJ and Lee JH: Performance of CT in the preoperative diagnosis of cervical lymph node metastasis in patients with papillary thyroid cancer: A systematic review and meta-analysis. AJNR Am J Neuroradiol 38: 154-161, 2017.
18. Traylor KS: Computed tomography and MR imaging of thyroid disease. Radiol Clin North Am 58: 1059-1070, 2020.
19. Yoo RE, Kim JH, Hwang I, Kang KM, Yun TJ, Choi SH, Sohn CH and Park SW: Added value of computed tomography to ultrasonography for assessing LN metastasis in preoperative patients with thyroid cancer: Node-by-node correlation. Cancers (Basel) 12: 1190, 2020.
20. Jeon YH, Lee JY, Yoo RE, Rhim JH, Lee KH, Choi KS, Hwang I, Kang KM and Kim JH: Validation of ultrasound and computed tomography-based risk stratification system and biopsy criteria for cervical lymph nodes in preoperative patients with thyroid cancer. Korean J Radiol 24: 912-923, 2023.
21. Feng Y, Min Y, Chen H, Xiang K, Wang X and Yin G: Construction and validation of a nomogram for predicting cervical lymph node metastasis in classic papillary thyroid carcinoma. J Endocrinol Invest 44: 2203-2211, 2021.
22. Li J, Sun P, Huang T, Li L, He S, Ai X, Xiao H and Xue G: Preoperative prediction of central lymph node metastasis in cN0T1/T2 papillary thyroid carcinoma: A nomogram based on clinical and ultrasound characteristics. Eur J Surg Oncol 48: 1272-1279, 2022.
23. Yang Z, Heng Y, Lin J, Lu C, Yu D, Tao L and Cai W: Nomogram for predicting central lymph node metastasis in papillary thyroid cancer: A retrospective cohort study of two clinical centers. Cancer Res Treat 52: 1010-1018, 2020.
24. Edge SB, Byrd DR, Compton CC, Fritz AG, Greene FL and Trotti A (eds): AJCC Cancer staging handbook: from the AJCC cancer staging manual. 7th edition. Springer-Verlag, New York, NY, 2010.
25. Coca-Pelaz A, Shah JP, Hernandez-Prera JC, Ghossein RA, Rodrigo JP, Hartl DM, Olsen KD, Shaha AR, Zafereo M, Suarez C, *et al*: Papillary thyroid cancer-aggressive variants and impact on management: A narrative review. Adv Ther 37: 3112-3128, 2020.
26. Lee YM, Sung TY, Kim WB, Chung KW, Yoon JH and Hong SJ: Risk factors for recurrence in patients with papillary thyroid carcinoma undergoing modified radical neck dissection. Br J Surg 103: 1020-1025, 2016.
27. Feng JW, Hong LZ, Wang F, Wu WX, Hu J, Liu SY, Jiang Y and Ye J: A nomogram based on clinical and ultrasound characteristics to predict central lymph node metastasis of papillary thyroid carcinoma. Front Endocrinol (Lausanne) 12: 666315, 2021.
28. Gao X, Luo W, He L, Cheng J and Yang L: Predictors and a prediction model for central cervical lymph node metastasis in papillary thyroid carcinoma (cN0). Front Endocrinol (Lausanne) 12: 789310, 2021.
29. Luo QW, Gao S, Lv X, Li SJ, Wang BF, Han QQ, Wang YP, Guan QL and Gong T: A novel tool for predicting the risk of central lymph node metastasis in patients with papillary thyroid microcarcinoma: A retrospective cohort study. BMC Cancer 22: 606, 2022.
30. Gui CY, Qiu SL, Peng ZH and Wang M: Clinical and pathologic predictors of central lymph node metastasis in papillary thyroid microcarcinoma: A retrospective cohort study. J Endocrinol Invest 41: 403-409, 2018.
31. Li X, Zhang H, Zhou Y and Cheng R: Risk factors for central lymph node metastasis in the cervical region in papillary thyroid carcinoma: A retrospective study. World J Surg Oncol 19: 138, 2021.
32. Wang Z, Chang Q, Zhang H, Du G, Li S, Liu Y, Sun H and Yin D: A clinical predictive model of central lymph node metastases in papillary thyroid carcinoma. Front Endocrinol (Lausanne) 13: 856278, 2022.
33. Zhao S, Yue W, Wang H, Yao J, Peng C, Liu X and Xu D: Combined conventional ultrasound and contrast-enhanced computed tomography for cervical lymph node metastasis prediction in papillary thyroid carcinoma. J Ultrasound Med 42: 385-398, 2023.
34. Lee JH, Kim Y, Choi JW and Kim YS: The association between papillary thyroid carcinoma and histologically proven Hashimoto's thyroiditis: A meta-analysis. Eur J Endocrinol 168: 343-349, 2013.
35. Wang Y, Zheng J, Hu X, Chang Q, Qiao Y, Yao X and Zhou X: A retrospective study of papillary thyroid carcinoma: Hashimoto's thyroiditis as a protective biomarker for lymph node metastasis. Eur J Surg Oncol 49: 560-567, 2023.
36. Issa PP, Omar M, Buti Y, Issa CP, Chabot B, Carnabatu CJ, Munshi R, Hussein M, Aboueisha M, Shama M, *et al*: Hashimoto's thyroiditis minimizes lymph node metastasis in BRAF mutant papillary thyroid carcinomas. Biomedicines 10: 2051, 2022.
37. Jara SM, Carson KA, Pai SI, Agrawal N, Richmon JD, Prescott JD, Dackiw A, Zeiger MA, Bishop JA and Tufano RP: The relationship between chronic lymphocytic thyroiditis and central neck lymph node metastasis in North American patients with papillary thyroid carcinoma. Surgery 154: 1272-1280, 2013.
38. Mao J, Zhang Q, Zhang H, Zheng K, Wang R and Wang G: Risk factors for lymph node metastasis in papillary thyroid carcinoma: A systematic review and meta-analysis. Front Endocrinol (Lausanne) 11: 265, 2020.
39. Liu Y, Lv H, Zhang S, Shi B and Sun Y: The impact of coexistent Hashimoto's thyroiditis on central compartment lymph node metastasis in papillary thyroid carcinoma. Front Endocrinol (Lausanne) 12: 772071, 2021.
40. Sun J, Jiang Q, Wang X, Liu W and Wang X: Nomogram for preoperative estimation of cervical lymph node metastasis risk in papillary thyroid microcarcinoma. Front Endocrinol (Lausanne) 12: 613974, 2021.
41. Li Y, Gao X, Guo T and Liu J: Development and validation of nomograms for predicting the risk of central lymph node metastasis of solitary papillary thyroid carcinoma of the isthmus. J Cancer Res Clin Oncol 149: 14853-14868, 2023.
42. Lyu YS, Pyo JS, Cho WJ, Kim SY and Kim JH: Clinicopathological significance of papillary thyroid carcinoma located in the isthmus: A meta-analysis. World J Surg 45: 2759-2768, 2021.
43. Zhu F, Li F, Xie X, Wu Y and Wang W: Investigating the impact of tumor location and size on the risk of recurrence for papillary thyroid carcinoma in the isthmus. Cancer Med 12: 13290-13299, 2023.

44. Schmitz G and Dencks S: Ultrasound imaging. Recent Results Cancer Res 216: 135-154, 2020.
45. Bin Saeedan M, Aljohani IM, Khushaim AO, Bukhari SQ and Elnaas ST: Thyroid computed tomography imaging: Pictorial review of variable pathologies. Insights Imaging 7: 601-617, 2016.
46. Tian X, Song Q, Xie F, Ren L, Zhang Y, Tang J, Zhang Y, Jin Z, Zhu Y, Zhang M and Luo Y: Papillary thyroid carcinoma: An ultrasound-based nomogram improves the prediction of lymph node metastases in the central compartment. Eur Radiol 30: 5881-5893, 2020.
47. Pyo JS, Kang G, Kim DH, Park C, Kim JH and Sohn JH: The prognostic relevance of psammoma bodies and ultrasonographic intratumoral calcifications in papillary thyroid carcinoma. World J Surg 37: 2330-2335, 2013.
48. Ferreira LB, Lima RT, Bastos ACSDF, Silva AM, Tavares C, Pestana A, Rios E, Eloy C, Sobrinho-Simões M, Gimba ERP and Soares P: OPNa overexpression is associated with matrix calcification in thyroid cancer cell lines. Int J Mol Sci 19: 2990, 2018.
49. Li X, Zhou W and Zhan W: Clinical and ultrasonographic features of medullary thyroid microcarcinomas compared with papillary thyroid microcarcinomas: A retrospective analysis. BMC Med Imaging 20: 49, 2020.
50. Liu J, Jia X, Gu Y, Chen X, Guan L, Yan J, Zhai H, Zhou N, Dong Y, Zhan W, *et al*: Thyroid parenchyma microcalcifications on ultrasound for predicting lymph node metastasis in papillary thyroid carcinoma: A prospective multicenter study in China. Front Oncol 11: 609075, 2021.
51. Lugano R, Ramachandran M and Dimberg A: Tumor angiogenesis: Causes, consequences, challenges and opportunities. Cell Mol Life Sci 77: 1745-1770, 2020.
52. Zhang F, Qiao Y and Zhang H: Value of CT features in the diagnosis of papillary thyroid tumors in incidental thyroid nodules. Int J Endocrinol 2020: 9342317, 2020.
53. Park JP, Roh JL, Lee JH, Baek JH, Gong G, Cho KJ, Choi SH, Nam SY and Kim SY: Risk factors for central neck lymph node metastasis of clinically noninvasive, node-negative papillary thyroid microcarcinoma. Am J Surg 208: 412-418, 2014.
54. Peng Y, Zhang ZT, Wang TT, Wang Y, Li CH, Zuo MJ, Lin HS and Gong LG: Prediction of central lymph node metastasis in cN0 papillary thyroid carcinoma by CT radiomics. Acad Radiol 30: 1400-1407, 2023.
55. Mou Y, Han X, Li J, Yu P, Wang C, Song Z, Wang X, Zhang M, Zhang H, Mao N and Song X: Development and validation of a computed tomography-based radiomics nomogram for the preoperative prediction of central lymph node metastasis in papillary thyroid microcarcinoma. Acad Radiol 31: 1805-1817, 2023.